III　画像検査

6. びまん性肺疾患の CT 診断の進歩

Key words：びまん性肺疾患，慢性閉塞性肺疾患，特発性間質性肺炎，多列検出器 CT（MDCT），3 次元高分解能データ解析/diffuse parenchymal lung disease, chronic obstructive pulmonary disease (COPD), idiopathic interstitial pneumonia (IIP), multidetector CT (MDCT), volumetric data analysis

藤本公則*,**

要　旨

びまん性肺疾患の CT 診断は，最近の CT 技術の進歩により，高分解能 CT を用いた肺小葉レベルの所見解析のような微細形態診断に加え，MDCT による高速撮像や volumetric data 取得が可能となって，呼吸運動を利用した動態解析や多方向断面による微細構造の観察や測定，CT 値を利用した定量評価などが新たに行われるようになってきた。今後は疾患別に種々の解析法を駆使していくことになるが，これらの情報をどのように臨床の現場に還元していくかが重要である。

はじめに

概して，びまん性肺疾患は胸部単純 X 線写真でびまん性陰影を呈する疾患の総称であり，多種多様な疾患，病因を包括する。

びまん性肺疾患における CT 診断の進歩としては，CT 技術の進歩と疾患に対する CT 所見解析の進歩に大きく分けられる。CT 技術の進歩として，高分解能 CT，螺旋スキャンの開発と多列検出器 CT（multidetector CT：MDCT）によって大量の連続データ取得が可能になったこと，コンピュータの発達により高精細で種々の解析が可能になったことなどが挙げられ，特に慢性閉塞性肺疾患（chronic obstructive pulmonary disease：COPD）における CT データを用いた各種解析法の重要性が挙げられる[1]。疾患に対する CT 所見解析の進歩としては，高分解能 CT における末梢肺野構造の解剖学的な理解，特に Miller の 2 次小葉を基本とした所見解析法[2)3)]が広く理解されるに至り，膨大な検討結果とエビデンスが蓄積され，特に特発性間質性肺炎（idiopathic interstitial pneumonias：IIPs）の診断における臨床-画像-病理（clinical-radiological-pathological：C-R-P）診断の重要性が認識され，その診断基準，鑑別診断に CT 所見が組み込まれた[4]ことが挙げられる。

本稿では，びまん性肺疾患のうち慢性閉塞性肺疾患と特発性間質性肺炎における CT 診断について，前述の CT の進歩という点を中心に概説し，その研究の一部を紹介する。

慢性閉塞性肺疾患の CT 診断

1. COPD の気腫病変の評価

気腫病変の CT による評価法としては，気腫腔と判定する低吸収域（low attenuation area：LAA）の CT 値（Hounsfield unit：HU）の閾値を設定して強調し，肺野全体に占める LAA の範囲を評価する方法（density mask program）[5]が一般的で，主に上・中・下肺野の代表とする CT 横断画像における LAA の占める程度を視覚的にグレーディング（ランク分け）する半定量的方法は，気道の閉塞性障害を示す呼吸機能検査と相関性が高い[6]ことが知られている。その後，気腫腔と判定する LAA の CT 値の閾値を決定し，その領域をコンピュータ解析で呼び出して面積を計算し，肺野全体の面積で除し，LAA％として評価する方法[7]のほうが定量性，客観性，再現性に優れ，コンピュータ自動解析も行いうる客観的定量評価法として報告された。最近ではより精度の高い方法を目指して，volumetric data を用い立体的に評価することも一般的となりつつある（図 1）。自動解析によっ

Multidetector CT Diagnosis for Diffuse Parenchymal Lung Diseases：Up to Date

Kiminori FUJIMOTO**

* *Department of Radiology, Kurume University School of Medicine and* ** *Center for Diagnostic Imaging, Kurume University Hospital, Kurume*

* 久留米大学医学部放射線科（〒830-0011　福岡県久留米市旭町 67）

** 久留米大学病院画像診断センター

Computed Tomographic Findings and Prognosis in Thymic Epithelial Tumor Patients

Satomi Yakushiji, MD, Ukihide Tateishi, MD, PhD,† Shunji Nagai, MD,† Yoshihiro Matsuno, MD, PhD,‡ Kazuo Nakagawa, MD, PhD,§ Hisao Asamura, MD, PhD,§ and Masahiko Kusumoto, MD, PhD†*

Objective: To determine which computed tomographic findings are associated with high-risk thymic epithelial tumors and a poor prognosis.

Methods: Computed tomographic findings of thymic epithelial neoplasms were retrospectively evaluated in 75 patients diagnosed with thymic tumor between January 1997 and October 2003. We analyzed the correlation of the computed tomographic findings, histological subtype according to the World Health Organization classification, and the prognosis.

Results: There were 34 with type A ~B1 tumor and 41 with type B2 ~ C tumor. On multiple regression analysis, vascular obliteration and a blunt sternum-anterior mediastinum angle were more frequent with thymic carcinoma than with thymoma. On multivariate analysis, pleural effusion and mediastinal fat infiltration on initial computed tomography had a significant impact on survival.

Conclusions: Vascular obliteration and a blunt sternum-anterior mediastinum angle were predictive of thymic carcinoma. Pleural effusion and mediastinal fat infiltration were predictive of a poor prognosis.

Key Word: thymic epithelial tumors, CT finding

(*J Comput Assist Tomogr* 2008;32:799–805)

Thymic epithelial tumors are uncommon and have a broad spectrum of biological and morphological features. Therefore, various histological classifications and staging systems have been devised to clarify the prognostic features of these tumors.

In 1999, the World Health Organization (WHO) published its histological classification of thymic tumors.[1] Several studies have evaluated the clinical and prognostic relevance of this histological classification. Recently, it has been reported that the WHO histological classification reflects both the clinical and the functional features of thymic epithelial tumors and is thus useful in clinical practice for both assessment and treatment.[2–4] It has been found that type A, AB, and B1 thymomas have a less aggressive nature than type B2 and B3 thymomas.[2,4–6]

Only a few studies have attempted to preoperatively predict the prognosis of these tumors based on computed tomography and pathological findings.[7–10] These studies found that there is some degree of overlap between the computed tomographic (CT) findings for the various histological types of tumors in the WHO classification. Thus, these reports concluded that computed tomography is of limited value in differentiating among the various histological subtypes. However, some CT findings of thymic epithelial tumors may help to differentiate the various subtypes and predict prognosis, but there have been few studies that have evaluated the relationship between the CT findings of thymic epithelial tumors and prognosis.[10]

The purpose of our study was to determine which CT findings of thymic epithelial tumors were associated with the high-risk group and a poor prognosis.

MATERIALS AND METHODS

Patients and Pathological Evaluation

We conducted a retrospective review of 77 patients who were diagnosed as having thymic epithelial tumors on pathology between January 1997 and October 2003. Two of 77 patients for whom initial CT scans were not available were excluded. Therefore, 75 patients with thymic epithelial tumors were considered. The medical records were reviewed with respect to clinicopathologic issues, including allied diseases, type of operation, adjuvant therapy, mode of recurrence, and prognosis.

In 52 patients, the diagnosis was made on the basis of surgical resection (total thymectomy, 36; thymectomy, 14); in the remaining 23 patients, the diagnosis was made on biopsy (percutaneous core needle biopsy, 21; exploratory surgery, 2). For the patients who were diagnosed on biopsy, other primary sites were excluded by laboratory tests (including serum tumor markers) and CT scan of other sites.

All tumors were staged according to the Masaoka clinicopathologic staging system.[11] This staging system incorporates the presence of invasion and the anatomical extent of involvement as defined clinically and histopathologically. The stage was determined by a review of the medical records, including operative, pathological, and radiological reports.

The mean follow-up period was 28 months (range, 1–87 months). For surgically treated patients, recurrence was defined as any evidence of tumor detected by imaging or pathological examination during follow-up.

The pathological specimens that were obtained before 2000 were reviewed and reclassified according to the 1999 WHO classification by an experienced pathologist.[6] From 2001, the pathological reports were based on the 1999 WHO classification so we can easily review those records. The

From the *Divisions of Medical Oncology; †Diagnostic Radiology; ‡Diagnostic Pathology, and §Thoracic Surgery, National Cancer Center Hospital and Research Institute, Tokyo, Japan.

Received for publication July 10, 2007; accepted July 27, 2007.

Reprints: Masahiko Kusumoto, MD, PhD, Division of Diagnostic Radiology, National Cancer Center Hospital, 1-1 Tsukiji 5-Chome, Chuo-ku, Tokyo 104-0045, Japan (e-mail: mkusumot@ncc.go.jp).

classification is as follows. Type A is a tumor composed of a population of spindle or oval neoplastic thymic epithelial cells lacking unclear atypia and accompanied by few or no neoplastic lymphocytes. Type AB is a tumor in which there are foci rich in lymphocytes. Type B1 is a tumor that resembles the normal functional thymus in that it combines large areas practically indistinguishable from normal thymic cortex with areas resembling thymic medulla. Type B2 is a tumor in which the neoplastic epithelial component appears as scattered plump cells with vesicular nuclei and distinct nucleoli among a large population of lymphocytes; perivascular spaces are common and sometimes very prominent, and there is a perivascular arrangement of tumor cells resulting in a pallisading effect. Type B3 is a type of thymoma predominantly composed of round or polygonal epithelial cells exhibiting no or mild atypia admixed with a minor component of lymphocytes, resulting in a sheetlike growth of the neoplastic epithelial cells. Type C is a type of thymoma exhibiting clear-cut cytological atypia and a set of cytoarchitectural features no longer specific to the thymus but rather analogous to those seen in carcinomas of other organs. All thymic carcinomas are classified as type C.

All tumors were grouped into 3 subgroups: low-risk thymomas (types A , AB, and B1), high-risk thymomas (types B2 and B3), and thymic carcinoma (type C).[10] For analysis, we compared the low-risk group (low-risk thymomas) to the high-risk group (high-risk thymomas and thymic carcinoma).

Image Acquisition and Analysis

Computed tomographic scans were available for 75 patients. Computed tomographic scans were taken before any therapy was given except in 2 patients who had been given chemotherapy at another hospital. The mean interval between pathological diagnosis and CT scan was 21 days (range, 0–201 days). Three patients were scanned at other hospitals.

Computed tomographic examination with a helical scanner (TCT-900S or X-Vigor; Toshiba Medical Systems, Tokyo, Japan) and a multislice CT scanner (Aquilion; Toshiba Medical Systems) was done in all patients. The helical technique in all patients consisted of 7.0- to 10.0-mm collimation for individual scans of the entire thorax (120 kVp, 150-200 mA per real EC) and reconstruction with a standard algorithm. Additional thin-section CT images were obtained in all patients using 2.0-mm collimation, a 20-cm field of view, 120 kVp, and 200 mA per rotation, 1.0- or 0.5-second gantry rotation, and a standard reconstruction algorithm. Computed tomographic examinations were performed 40 seconds after intravenous administration of 300 mg/mL of nonionic contrast material (Ipamiron 300; Nihon Schering K.K., Osaka, Japan) given at 2 to 3 mL/s. Hard copy photographic images were acquired at window settings for the mediastinum (center, 55 Hounsfield units; width, 550 Hounsfield units).

Two chest radiologists who were blinded to the histological classifications and tumor prognoses assessed the CT scans retrospectively. Decisions on the findings were reached by consensus. The CT analysis included the size (short and long axes), shape, marginal characteristics, enhancement pattern and degree compared with chest wall muscle, and the presence of calcification. The presence of mediastinal fat infiltration, invasion and obliteration of the great vessels, invasion of bone, pleural and pericardial effusion, pleural metastases, pleural dissemination, lymph node enlargement, and distant metastases were also evaluated. In particular, we evaluated the retrosternal marginal shapes of the tumor and described the "sternum-anterior mediastinum angle" as either blunt or sharp (Figs. 1, 2, and 4).

The longest diameter of the tumor was measured at the level where the axial tumor image seemed largest. The shape was classified as round if the long- to short-axis ratio was less than 1.5, oval if the ratio was equal to 1.5 or greater and less than 3.0, and plaque-like if the ratio was equal to or greater than 3.0. Tumor margin characteristics were subdivided into smooth, lobulated, and irregular. The pattern of enhancement was recorded as homogeneous or heterogeneous, and the degree of enhancement was evaluated as less than that of chest wall muscle, equal to that of chest wall muscle, and higher than that of chest wall muscle based on a visual estimate. Invasion of the great vessels was considered to be present when the tumor abutted and altered the contour of the corresponding vessels or when overt tumor thrombosis and vascular occlusion were present.

Statistical Analysis

The differences in the prevalence of each CT finding for the different simplified WHO histological subgroups (low-risk group compared with high-risk group) were analyzed using the χ^2 test. To differentiate among low-risk thymoma (type A, AB, and B1 tumors), high-risk thymoma (type B2 and B3 tumors), and thymic carcinoma (type C tumors), multiple logistic regression analyses were done.

Survival time was calculated from the day of the first CT scan until death or the last follow-up day. The Kaplan-Meier

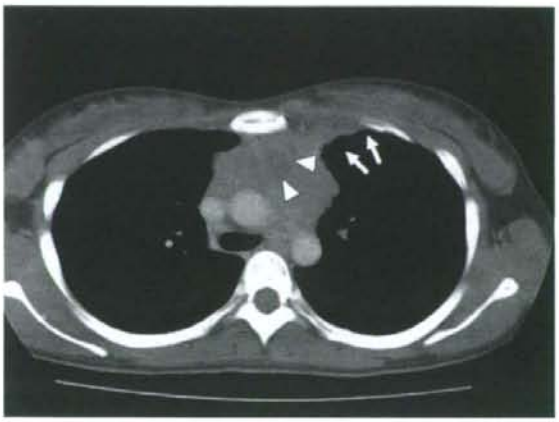

FIGURE 1. A 24-year-old woman with thymic carcinoma (type C). Enhanced CT scan (10-mm collimation) obtained at the level of the main trunk shows a 7.0 × 5.8–cm, oval, anterior mediastinal mass with a lobulated contour and a heterogeneous enhancement pattern (white arrowheads). This film shows that the sternum-anterior mediastinum angle was blunt (white arrow).

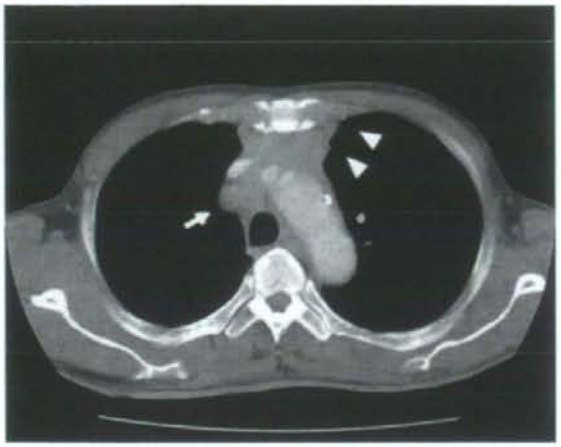

FIGURE 2. A 61-year-old man with thymic carcinoma (type C). Enhanced transaxial CT scan (10-mm collimation) obtained at the level of the aortic arch shows a 6.0 × 2.5–cm, oval, anterior mediastinal mass with a lobulated contour and a blunt sternum-anterior angle (white arrowheads). Also note the enlarged right paratracheal lymph node (white arrow).

method was used to estimate time to death from thymoma-related causes. All deaths that were not related to the thymic epithelial tumor were excluded from the calculation of survival curves. Deaths resulting from other causes were considered as censored. The differences in survival were tested by the log-rank test. Multivariate analysis using Cox proportional hazard regression model was performed to identify which CT findings were related to prognosis. The following variables were considered as possible prognostic CT findings: enhancement pattern, presence of vascular obliteration, blunt sternum-anterior mediastinal angle, lymph node metastasis, distant metastasis, pleural dissemination, pleural effusion, and mediastinal fat infiltration. These statistical analyses were done using SPSS software (version 11; SPSS, Inc, Chicago, Ill).

TABLE 1. The Relationship Between the Simplified WHO Classification[10] and Masaoka Clinical-Pathologic Staging[11]

Masaoka Clinicopathologic Staging	Low-Risk Group, Low-Risk Thymoma (A, AB, and B1; n = 34)	High-Risk Group: High-Risk Thymoma (B2 and B3; n = 15)	High-Risk Group: Thymic Carcinoma (C; n = 26)
1	11 (32)	1 (7)	0 (0)
2	17 (50)	6 (40)	2 (8)
3	3 (9)	3 (20)	4 (15)
4a	3 (9)*	4 (27)	3 (12)*
4b	0 (0)	0 (0)	16 (62)*

Numbers in parentheses are percentages.

Staging was not known for 1 patient each in the high-risk thymoma and thymic carcinoma groups.

*All of known were not treated surgically.

RESULTS

Clinicopathologic Findings

There were 37 men and 38 women who ranged in age from 24 to 80 years (mean age, 57 ± 11 years). Forty-four (59%) of the 75 patients were asymptomatic; their tumors had been detected incidentally by chest radiographs or CT scan. In the symptomatic patients, the most common symptoms were chest pain or discomfort (17/75; 23%), followed by cough (2/75; 16%), dyspnea (6/75; 8%), hoarseness (3/75; 4%), facial edema (2/75; 3%), dysphagia (1/75; 1%), and fever (1/75; 1%). Eight patients had other malignant disease: 3 had lung cancer, 2 had colon cancer, and 1 each had gastric cancer, breast cancer, or endometrial cancer. Four patients (5%) had allied diseases; myasthenia gravis occurred postoperatively in 3 patients (4%), and pure red cell aplasia occurred in 1 patient. Distant metastases were present in 8 patients; 5 of these had pulmonary metastases. Fifteen patients (20%) died of thymoma-related causes.

Of the patients who underwent surgery, 10 received perioperative chemotherapy, (preoperatively, 9 patients;

TABLE 2. CT Findings of Thymic Epithelial Tumors Based on Simplified WHO Classification[10]

CT Finding	Low-Risk Group: Low-Risk Thymoma (A, AB, B1; n = 34)	High-Risk Groups: High-Risk Thymoma (B2, B3; n = 15)	High-Risk Groups: Thymic Carcinoma (C; n = 26)
Size (cm)			
≤6	18 (53)	8 (53)	7 (27)
6	16 (47)	7 (47)	19 (73)
Contour*			
Smooth	23 (68)	7 (47)	3 (11.5)
Lobular	9 (26)	8 (53)	20 (77)
Irregular	2 (6)	0 (0)	3 (11.5)
Shape			
Round	20 (59)	7 (47)	15 (58)
Oval	12 (35)	6 (40)	11 (42)
Plaque	2 (6)	2 (13)	0 (0)
Calcification	4 (12)	4 (27)	5 (19)
Enhancement			
Homogeneous	19 (56)	11 (73)	11 (42)
Heterogeneous	10 (30)	3 (20)	15 (58)
Enhancement degree†			
Equal	2 (6)	1 (7)	2 (8)
Greater	27 (79)	13 (87)	24 (92)
Pleural effusion*	1 (3)	3 (20)	8 (31)
Vascular obliteration*	1 (3)	1 (7)	20 (77)
Blunt angle*	1 (3)	1 (7)	13 (50)
Mediastinal infiltration	4 (12)	0 (0)	7 (27)
LN*	1 (3)	0 (0)	12 (46)
Pleural dissemination*	2 (6)	3 (20)	6 (23)
Lung metastasis*	0 (0)	0 (0)	5 (19)

Numbers in parentheses are percentages.

Blunt angle indicates blunt sternum-anterior mediastinal angle; LN, lymph node metastasis.

*Differences from other tumor types were statistically significant ($P < 0.05$).

†Compared with that of chest wall muscle.

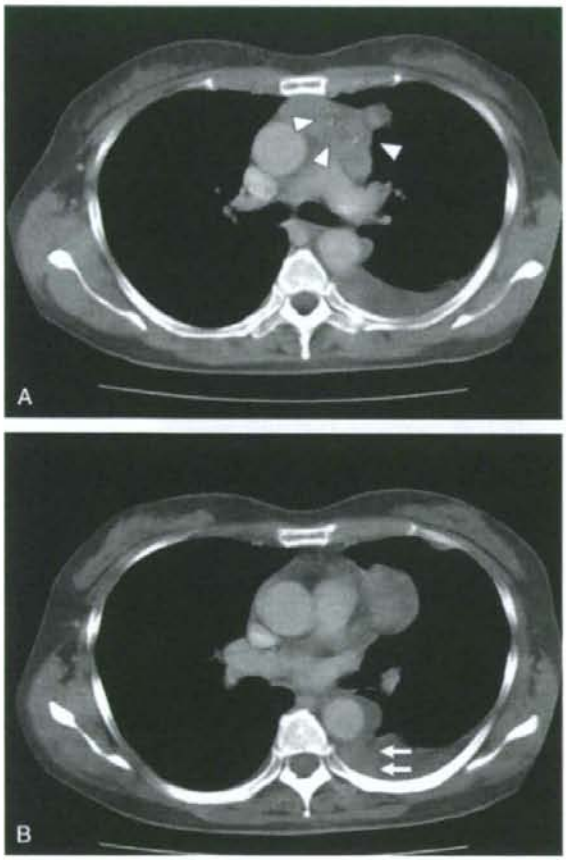

FIGURE 3. A 52-year-old woman with a high-risk thymoma (type B3 tumor). Enhanced transaxial CT scan (10-mm collimation) obtained at the level of the carina shows a 6.1 × 4.3–cm, plaque, anterior mediastinal mass with a lobulated contour and egg-like calcification (white arrowheads). The sternum-anterior mediastinum angle was sharp. This scan also shows a pleural effusion (A). Computed tomographic scan obtained at the level of the atrium shows a pleural effusion and nodular thickening of the pleura (white arrow), suggesting pleural tumor implantation (B).

postoperatively, 10 patients; both preoperatively and postoperatively, 1 patient). Eight patients received postoperative radiotherapy at 40 to 50 Gy. Of the patients who did not have surgery, 7 patients received chemotherapy, and 12 patients received both chemotherapy and radiotherapy.

There were 34 low-risk thymomas (4 type A tumors, 21 type AB, and 9 type B1), 15 high-risk thymomas (13 type B2 and 2 type B3), and 26 thymic carcinomas (type C). The relationship between Masaoka clinicopathologic stage and WHO classification is summarized in Table 1. The proportion of invasive tumors (stages II, III, IVa, and IVb Masaoka classification) showed a trend to increase according to tumor type; the lowest proportion was in low-risk thymomas, a higher proportion in high-risk thymomas, and the highest proportion of invasive tumors was in thymic carcinomas.

CT Findings

Based on the simplified WHO histological classification, CT finding of thymic epithelial tumors are summarized in Table 2. The long- and short-axis diameters (mean ± SD) of the tumors in the simplified WHO histological subgroups were long axis, 55.7 ± 24.8 mm and short axis, 36.8 ± 15.5 mm for low-risk thymomas; long axis, 58.5 ± 24.9 mm and short axis, 41.0 ± 16.1 mm for high-risk thymomas; and long axis, 72.4 ± 24.1 mm and short axis, 54.7 ± 20.3 mm for thymic carcinomas. Overall, the median long-axis diameter of the tumor was 60 mm. For analysis, therefore, we divided the patients into 2 groups based on their tumor's long-axis diameter: greater than 60 and 60 mm or less. There was no significant difference in the number of patients with a tumor long-axis diameter 60 mm or less between the low-risk (18/34; 53%) and the high-risk groups (15/41; 37%; P = 0.471). A lobulated contour was more often seen in the high-risk group (28/41; 68%; P = 0.0005) than in the low-risk group (9/34; 26%), but an irregular contour was seen both in the low-risk (all type B1 tumors) and the high-risk groups (all type C tumors) (Figs. 1–4). Calcification was seen both in the low-risk (4/12; 12%) and in the high-risk groups (9/41; 22%); the frequency of calcification was not significantly different between the low-risk and the high-risk groups (P = 0.246; Fig. 3). Pleural effusion (P = 0.005; Fig. 3), vascular obliteration (P < 0.0001; Fig. 4), blunt sternum-anterior mediastinum angle (P = 0.0008; Figs. 1, 2, 4), lymph node metastasis (P = 0.0027; Figs. 2, 4), and pleural dissemination

FIGURE 4. A 68-year-old woman with thymic carcinoma (type C thymoma). Enhanced transaxial CT scan (10-mm collimation) obtained at the level of the aortopulmonary window shows a 10.0 × 8.0–cm, heterogeneously enhancing anterior mediastinal mass with a lobulated contour. A blunt sternum-anterior mediastinum angle (white arrowheads), pulmonary arterial compression (white arrow), mediastinal involvement, and enlarged paratracheal lymph node can be seen.

TABLE 3. Univariate Analysis of 5-Year Survival Rate of Patients With Thymoma According to CT Findings

Covariables	n	5-Year Survival (%)	P
Size (cm)			
≤6	31	78.8	0.471
>6	44	66.87	
Shape			
Oval	29	72.00	0.8615
Plaque	4	66.67	
Round	42	72.81	
Contour			
Irregular	5	0	0.0022
Lobulate	37	65.6	
Smooth	33	85.74	
Enhancement pattern			
Homogeneous	41	90.12	0.0137
Heterogeneous	28	48.70	
Enhancement degree*			
Equal	5	40.00	0.2273
Greater	64	73.66	
Calcification			
Negative	62	72.36	0.8859
Positive	13	68.75	
Pleural effusion			
Negative	63	87.68	<0.0001
Positive	12	0	
Vascular obiliteration			
Negative	53	82.95	<0.0001
Positive	22	33.74	
Blunt angle			
Negative	60	83.52	<0.0001
Positive	15	19.23	
Mediastinal fat infiltration			
Negative	64	77.31	0.0008
Positive	11	38.18	
LN			
Negative	62	75.05	0.0872
Positive	13	50.14	
Pleural dissemination			
Negative	64	77.64	0.1078
Positive	11	35.00	

Blunt angle indicates blunt sternum-anterior mediastinal angle; LN, lymph node metastasis.
*Compared with that of chest wall muscle.

($P = 0.05$; Fig. 3) were significantly more frequent in the high-risk group. Mediastinal fat infiltration was seen in the low-risk (1 type AB thymoma, 3 type B1 thymomas; 4/34; 12%) and in the thymic carcinoma groups (7/41; 17%; $P = 0.5177$; Fig. 4). Lung metastasis was seen only in the thymic carcinomas (5/41; 12%; $P = 0.03$). There were no significant differences between the low-risk and the high-risk groups in other CT findings, including tumor shape ($P = 0.8579$), pattern of enhancement ($P = 0.3798$), and degree of enhancement ($P = 0.9239$).

Multiple logistic regression analysis was done to identify the CT findings that can differentiate between low risk and high-risk thymomas and thymic carcinoma (Tables 4A, B). Vascular obliteration (odds ratio, 58.4521; $P < 0.0001$) and a blunt sternum-anterior mediastinum angle (odds ratio, 13.7751; $P = 0.012$) were more often seen in thymic carcinoma than in thymoma (types A, AB, and B1-3). Pleural effusion (odds ratio, 14.098; $P = 0.01826$) and vascular obliteration (odds ratio, 37.511; $P = 0.000758$) were seen more often in the high-risk (high-risk thymoma and thymic carcinoma) than in the low-risk thymoma group.

Prognosis

The median follow-up time for all 75 patients was 28 months (range, 1–87 months). During the follow-up period, 19 deaths occurred. Fifteen patients (79%) died of tumor-related causes, and the remaining 4 patients died of other causes (primary lung cancer, 1; colon cancer, 1; endometrial cancer, 1; and suicide, 1). Sixteen patients had recurrent or metastatic disease on follow-up computed tomography. Two of the 16 patients with recurrence had undergone a complete resection, 3 had undergone an incomplete surgical resection, and in the remaining 11 patients, surgery had not been done (these patients were diagnosed by biopsy).

The 5-year overall survival rates based on the simplified histologic subtypes were 91% (low-risk thymoma), 83% (high-risk thymoma), and 27% (thymic carcinoma). Survival rate was significantly better in the low-risk group than in the high-risk group (log-rank test; $P < 0.0001$).

Univariate analysis of 5-year survival rate based on CT findings is shown in Table 3. The survival rate of patients who had an irregular contour ($P = 0.0022$), a heterogeneous enhancement pattern ($P = 0.0137$), pleural effusion ($P < 0.0001$), vascular obliteration ($P < 0.0001$), blunt sternum-anterior mediastinum angle ($P < 0.0001$), mediastinal fat infiltration ($P = 0.0008$), lymph node metastasis ($P = 0.082$), distant metastasis ($P = 0.05$), and pleural dissemination ($P = 0.1078$) was lower than that of patients who had none of these CT findings. Enhancement degree ($P = 0.2273$), calcification on initial computed tomography ($P = 0.8859$), age ($P = 0.3691$), and sex ($P = 0.0879$) were not associated with shorter survival.

TABLE 4. Analysis

Covariable	Odds Ratio	95% CI	P
A. Multiple Logistic Regression Analysis for Thymic Carcinoma (Type C) and Thymoma (Type A, AB, B1–3)			
Vascular obliteration	58.4521	9.8020–348.5675	<0.0001
Blunt angle	13.7751	1.7802–106.5911	0.011991
B. Multiple Logistic Regression Analysis for the High Risk Group (Type B2, B3, C) and the Low Risk Group (Type A, AB, B1)			
Covariable	Odds Ratio	95% CI	P
Pleural effusion	14.0981	1.5664–126.8913	0.018263
Vascular obliteration	37.5109	4.5499–309.2486	0.000758
C. Multivariate Analysis			
Variables	Risk Ratio	95% CI	P
Pleural effusion	13.229	3.350–52.242	<0.0001
Mediastinal fat infiltration	9.589	2.134–43.080	0.003

Blunt angle indicates blunt sternum-anterior mediastinal angle; CI, confidence intervals.

Multivariate Analysis

Multivariate analysis was done with 8 variables (heterogeneous enhancement pattern, pleural effusion, vascular obliteration, blunt sternum-anterior mediastinal angle, mediastinal involvement, lymph node metastasis, distant metastasis, and pleural dissemination), as shown in Table 4C. Tumor with pleural effusion on initial computed tomography was the most significant CT finding associated with poor survival (relative risk, 13.229; $P < 0.0001$). Tumor with mediastinal involvement was also significantly associated with poor survival (relative risk, 9.589; $P = 0.003$).

DISCUSSION

The WHO histological classification has been shown to reflect the clinical feature of thymic epithelial tumors and to correlate with prognosis.[2–4] Okumura et al reported that type A, AB, and B1 thymomas have a less aggressive nature than type B2, B3, and C thymoma, and therefore form a low-risk group. Thus, preoperative differentiation between these 2 groups (low-risk group, type A, AB, and B1 thymomas; high-risk group, type B2, B3, and C thymomas) is considered to be helpful in therapeutic decision making.

There is some degree of overlap in the CT findings among the various WHO classification subtypes of thymoma. Therefore, preoperative prediction of WHO histological subtypes based on the CT findings is considered to have limited value.[7–9] Tomiyama et al reported that a smooth contour and a round shape most strongly suggest type A tumors; an irregular contour and mediastinal lymphadenopathy most strongly suggest a type C tumor; and calcification suggests type B1, B2, and B3 tumors. On the other hand, Jeong et al concluded that only the tumor contour, mediastinal fat, and great vessel invasion can be used to differentiate between low-risk and high-risk groups.

In this study, tumor contour, pleural effusion, vascular obliteration, a blunt sternum-anterior mediastinum angle, mediastinal fat infiltration, and lymphadenopathy enabled us to differentiate between the high-risk and low-risk groups. Although there are some differences with respect to the samples, overall, our results are similar to those previously published by Tomiyama et al[7] Jung et al,[8] and Jeong et al.[10] According to the present multilogistic analysis, vascular obliteration and pleural effusion were more useful in differentiating between the low-risk and high-risk groups than any other CT findings. In this study, we classified the sternum-anterior mediastinum angle as either blunt or sharp. A blunt sternum-anterior mediastinum angle on computed tomography may reflect the fact that, on pathology, tumor cells were invading into the mediastinal fat and chest wall. Therefore, a blunt sternum-anterior mediastinum angle on computed tomography would be indicative of more invasive tumor. In our study, a blunt sternum-anterior mediastinum angle was significantly more frequent in thymic carcinoma than in thymoma (odds ratio, 13.8; $P = 0.012$). This CT finding also helps to differentiate between thymic carcinoma and thymoma.

Many studies have attempted to identify the prognostic factors for thymic epithelial tumors. Although factors such as completeness of resection, tumor size, stage, and histology have been mentioned as prognostic factors in thymoma, the presence or absence of tumor invasion has been uniformly recognized as a prognostic factor.[6,12–20] Many studies have suggested that Masaoka staging and the WHO histological subtype should be recognized as factors that strongly affect the prognosis.[2–4,6,21,22] With respect to CT findings, Jeong et al reported that tumors with a lobulated or irregular contour, an oval shape, mediastinal fat or great vessel invasion, or pleural seeding showed significantly more frequent recurrence and metastases.[10] In our study, an irregular and lobular contour was seen in both the low-risk and high-risk groups; however, the prognosis for those who had an irregular and lobulate contour was poorer than for those who had a smooth contour ($P = 0.0022$). On univariate analysis, the presence of a heterogeneous enhancement pattern of the tumor ($P = 0.0137$), pleural effusion ($P < 0.0001$), vascular obliteration ($P < 0.0001$), a blunt sternum-anterior mediastinum angle ($P < 0.0001$), and mediastinal fat infiltration ($P = 0.008$) on the initial computed tomography were all significant risk factors for a poor prognosis (Table 3). Tomiyama et al[7] reported that calcifications within the tumor was suggestive of type B tumors. In our study, the frequency of calcification was not significantly different between the high-risk and low-risk groups ($P = 0.246$), and there were no significant differences in prognosis between patients who had calcification on computed tomography and those who did not.

On multivariate analysis, of all the CT findings, tumors with pleural effusions and mediastinal involvement on the initial computed tomography were most likely to have a poor prognosis. In the Masaoka staging system of thymoma, a pleural effusion would equal stage IVa.[11] However, the Masaoka staging system is postsurgical because the invasion of the capsule can only be reliably diagnosed on pathological examination. In our study, there were some patients who had a pleural effusion on initial computed tomography, and their prognosis was poorer than patients who did not have a pleural effusion on computed tomography. Therefore, a pleural effusion on the initial computed tomography can be considered to indicate a poor prognosis in patients with a thymic epithelial tumor.

Our study has some limitations. As with other studies, our study was not population based; thus, it could have been subject to selection bias. With respect to allied disease, the number of patients in our study who had myasthenia gravis (MG) was smaller than in other studies. Myasthenia gravis occurs in approximately 30% of patients with thymoma, and a host of paraneoplastic syndromes have been seen in association with thymoma.[23] This low number of MG patients in our study likely reflects the patient population of our institute because patients with MG symptoms tend to be treated in other hospitals. Our institute is a cancer center; thus, patients who have other allied disease were more likely to be treated in other hospitals too. On the other hand, the number of patients with thymic carcinoma was larger in our study than in other studies. Because most patients with thymic carcinoma were not treated surgically, their diagnoses were not as accurate as the patients who were treated surgically. Although we evaluated the overall survival rate, the follow-up period was not long enough to satisfactorily estimate prognosis. In addition, we examined

prognosis of these cases that therapeutic methods were different uniformly.

In conclusion, CT findings of vascular obliteration and a blunt sternum-anterior mediastinum angle were predictive of thymic carcinoma; pleural effusions and vascular obliteration were more frequent in the high-risk than in the low-risk thymoma group. Pleural effusions and mediastinal involvement on CT scan were related to a poor prognosis.

REFERENCES

1. Rosai J, Sovin LH. Histological typing of tumours of the thymus. In: *International Histological Classification of Tumours*. 2nd ed. New York, NY: Springer; 1999:5–14.
2. Okumura M, Miyoshi S, Fujii Y, et al. Clinical and functional significance of WHO classification on human thymic epithelial neoplasms: a study of consecutive 146 tumors. *Am J Surg Pathol*. 2001;25:103–110.
3. Chen G, Marx A, Wen-Hu C, et al. New WHO histologic classification predicts prognosis of thymic epithelial tumors: a clinicopathologic study of 200 thymoma cases from China. *Cancer*. 2002;95:420–429.
4. Okumura M, Ohta M, Tateyama H, et al. The World Health Organization histologic classification system reflects the oncological behavior of thymoma: a clinical study of 273 patients. *Cancer*. 2002;94:623–632.
5. Rieker RJ, Hoegel J, Morresi-Hauf A, et al. Histologic classification of thymic epithelial tumors: comparison of established classification schemes. *Int J Cancer*. 2002;98:900–906.
6. Nakagawa K, Asamura H, Matsuno Y, et al. Thymoma: a clinicopathologic study based on the new World Health Organization classification. *J Thorac Cardiovasc Surg*. 2003;126:1134–1140.
7. Tomiyama N, Johkoh T, Mihara N, et al. Using the World Health Organization classification of thymic epithelial neoplasms to describe CT findings. *AJR Am J Roentgenol*. 2002;179:881–886.
8. Jung KJ, Lee KS, Han J, et al. Malignant thymic epithelial tumors: CT-pathologic correlation. *AJR Am J Roentgenol*. 2001;176:433–439.
9. Han J, Lee KS, Yi CA, et al. Thymic epithelial tumors classified according to a newly established WHO schema: CT and MR findings. *Korean J Radiol*. 2003;4:46–53.
10. Jeong YJ, Lee KS, Kim H, et al. Does CT of thymic epithelial tumors enable us to differentiate histologic subtypes and predict prognosis? *AJR Am J Roentgenol*. 2004;183:283–289.
11. Masoka A, Monden Y, Nakahara K, et al. Follow-up study of thymomas with special reference to their clinical stages. *Cancer*. 1981;48:2485–2492.
12. Intanilla-Martinez L, Wilkins EW Jr, Shoi N, et al. Thymoma. Histologic subclassification is an independent prognostic factor. *Cancer*. 1994;74: 606–617.
13. Maggi G, Casadio C, Cavallo A, et al. Thymoma: results of 241 operated cases. *Ann Thorac Surg*. 1991;51:152–156.
14. Lardinois D, Rechsteiner R. Prognostic relevance of Masaoka and Muller-Hermelink classification in patients with thymic tumors. *Ann Thorac Surg*. 2000;69:1550–1555.
15. Pan CC, Wu HP, Yang CF, et al. The clinicopathological correlation of epithelial subtyping in thymoma: a study of 112 consecutive cases. *Hum Pathol*. 1994;25:893–899.
16. Shimosato Y. Controversies surrounding the subclassification of thymoma. *Cancer*. 1994;74:542–544.
17. Moran CA, Suster S. Thymoma atypical thymoma, and thymic carcinoma. A novel conceptual approach to the classification of thymic epithelial neoplasms. *Am J Clin Pathol*. 1999;111:826–833.
18. Blumberg D, Port JL, Weksler B, et al. Thymoma: a multivariate analysis of factors predicting survival. *Ann Thorac Surg*. 1995;60:908–913.
19. Regnard J-F, Magdeleinat P, Dromer C. Prognostic factors and long-term results after thymoma resection: a series of 307 patients. *J Thorac Cardiovasc Surg*. 1996;112:376–384.
20. Wilkins KB, Sheikh E, Green R, et al. Clinical and pathologic predictors of survival in patients with thymoma. *Ann Surg*. 1999;230:562–572.
21. Rios A, Torres J, Galindo PJ, et al. Prognostic factors in thymic epithelial neoplasms. *Eur J Cardiothorac Surg*. 2002;21:307–313.
22. Kim DJ, Yang WI, Shoi SS, et al. Prognostic and clinical relevance of the World Health Organization schema for the classification of thymic epithelial tumors. *Chest*. 2005;127:755–761.
23. Thomas CR Jr, Wright CD, Loehrer PJ. Thymoma: state of the art. *J Clin Oncol*. 1999;17:2280–2289.

診療の秘訣

アスベストによる胸膜中皮腫早期病変を見逃さないために

岸本　卓巳
岡山労災病院副院長・内科

アスベストによって発生する中皮腫が社会問題化している．中皮腫の80%以上を占める胸膜中皮腫は呼吸困難や胸痛を主訴として来院し，確定診断される場合が多い．しかし，自覚症状で来院した場合にはほとんどが進行期病変である．われわれが平成17年度から行った中皮腫の過去症例の追跡調査では，自覚症状がなく健康診断で胸水を指摘され，経過観察されていたり，結核性胸膜炎として治療されている間に画像上典型的な胸膜中皮腫像を呈したため，確定診断に至った症例が少なくないことが判明した．また，74%には職業性石綿ばく露を認めており，日本の中皮腫も石綿ばく露によって発生していることを確認した．

現時点では，胸膜中皮腫の有効な治療方法がなく，早期病変をきちんと診断して胸膜肺全摘出術を行うことが中皮腫の予後を改善する唯一の方法である．

胸部画像上，胸水を呈する患者を診療する際に注意することは，アスベストを直接あるいは間接的に職業上で使用したことがあるかどうか，また，家庭や環境でばく露した形跡がないかなどについて詳細な問診を行うことである．また，必ず胸部CTを撮影し，アスベストによる胸膜プラークの存在の有無を確認する．たとえ，腫瘍性胸膜肥厚や腫瘤がなくても，縦隔側胸膜の肥厚像は中皮腫の比較的早期病変である可能性があるので，必ず確認しておく（図）．

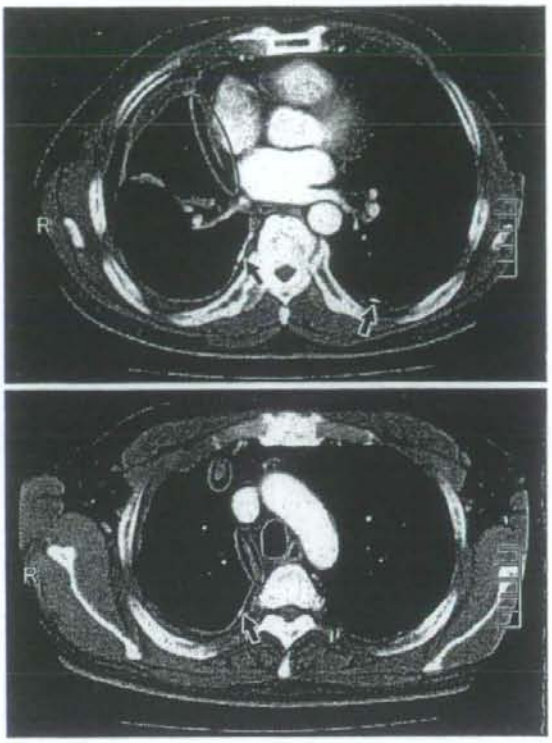

図
右縦隔側の胸膜肥厚像（赤丸印）が，中皮腫による変化である．この部位には脂肪層が認められるのみであるから，石灰化胸膜プラーク（黒矢印）が認められるような症例の場合，この程度の肥厚でも胸膜中皮腫を疑うべきである

胸水が穿刺によって検査ができる程度に貯留している場合には，試験穿刺を行って，その性状とともに，CEA，ADA，CYFRA21-1，ヒアルロン酸の測定と細胞診を行っておく．細胞診はパパニコロウ染色のみならず，cell peletsを作成し，カルレチニン，CEAなどを使用した免疫染色も行っておく．細胞診で胸膜中皮腫を診断できる可能性は40%以下であることを十分認識しておく．胸水中CEAが低値で，ヒアルロン酸が10万ng/ml以上あるいはCYFRA21-1が50 ng/ml以上の場合には，胸部画像上腫瘍性胸膜肥厚が認められない場合でも，胸腔鏡を行い壁側胸膜の観察と生検を行っておくべきである．生検はできるだけ大きく，深く採取することが確定診断上重要である．隆起性病変を認めない場合には，胸膜下を腫瘍が進展する肥厚型である場合もあるので，胸壁が透けて見えない場合にはその部位は必ず生検

0913-7963/08/¥800/論文/JCLS

しておく．万一，中皮腫であるとは診断できなかった場合にも，原因が不明で，職業性石綿ばく露がある場合には良性石綿胸水と診断される場合もあり，労災補償の対象となる場合には申請を行う．

胸水がわずかで，穿刺できないときは経過を慎重に追うことが重要であり，増加する場合には胸膜中皮腫の可能性も念頭においておく．

Immunological Changes in Mesothelioma Patients and Their Experimental Detection

Megumi Maeda[1], Yoshie Miura[1], Yasumitsu Nishimura[1], Shuko Murakami[1], Hiroaki Hayashi[1], Naoko Kumagai[1], Tamayo Hatayama[1], Minako Katoh[1], Naomi Miyahara[1], Shoko Yamamoto[1], Kazuya Fukuoka[2], Takumi Kishimoto[3], Takashi Nakano[2] and Takemi Otsuki[1]

[1]Department of Hygiene, Kawasaki Medical School, 577 Matsushima, Kurashiki 7010192, Japan. [2]Department of Respiratory Medicine, Hyogo Medical College of Medicine, 1-1 Mukogawa-cho, Nishinomiya, 6638131, Japan. [3]Okayama Rosai Hospital, 1-10-25 Chikkou-midori-machi, Okayama 7028055, Japan.

Abstract: It is common knowledge that asbestos exposure causes asbestos-related diseases such as asbestosis, lung cancer and malignant mesothelioma (MM) not only in people who have handled asbestos in the work environment, but also in residents living near factories that handle asbestos. These facts have been an enormous medical and social problem in Japan since the summer of 2005. We focused on the immunological effects of asbestos and silica on the human immune system. In this brief review, we present immunological changes in patients with MM and outline their experimental detection. For example, there is over-expression of *bcl-2* in CD4+ peripheral T-cells, high plasma concentrations of interleukin (IL)-10 and transforming growth factor (TGF)-ß, and multiple over-representation of T cell receptor (TcR)-Vß in peripheral CD3+ T-cells found in MM patients. We also detail an experimental long-term exposure T-cell model. Analysis of the immunological effects of asbestos may help our understanding of the biological effects of asbestos.

Keywords: asbestos, immunology, mesothelioma, chrysotile

Introduction

It is common knowledge that asbestos exposure causes asbestos-related diseases such as asbestosis, lung cancer and malignant mesothelioma (MM) not only in people who have handled asbestos in the work environment, but also in residents living near factories that handle asbestos. These facts have been an enormous medical and social problem in Japan since the summer of 2005 (Kanazawa et al. 2006; Murayama et al. 2006; Nakano, 2006). Several patients with MM living in Amagasaki, Hyogo prefecture, Japan have featured in news reports. These patients resided 1 km from an asbestos factory and had no identifiable occupational exposure to asbestos. Given that MM is an incurable disease and prognosis is not promising (Vogelzang and Pass, 2006; Zucali and Giaccone, 2006; Tsiouris and Walesby, 2007), and considering the absence of effective government legislation concerning the usage of asbestos, people in Japan have become concerned about social and medical issues related to asbestos.

Asbestos is categorized as a silicate (mineralogical complexes containing metals, such as iron and magnesium) and includes forms such as chrysotile, crocidolite, and amosite. Patients exposed to asbestos develop pulmonary fibrosis known as asbestosis, mesothelial plaque and malignant diseases such as lung cancer and MM (Niklinski et al. 2004; Becklake et al. 2007; O'Reilly et al. 2007). The mechanisms of asbestos-induced carcinogenesis are thought to produce an accumulation of DNA damage due to asbestos-induced production of reactive oxygen/nitrogen species (ROS/RNS) and an escape from the asbestos-induced activation of the mitochondrial apoptotic pathway (Shukla et al. 2003; Upadhyay and Kamp, 2003). In addition, we believe that some of these malignancies may be caused by a decline in tumor immunity owing to exposure of immunocompetent cells to asbestos.

Silica is known as one of the strongest environmental substances that cause autoimmunity dysfunction (Hess, 2002; Cooper and Parks, 2004). Silicosis patients often develop immunological complications such as rheumatic arthritis (known as Caplan syndrome (Caplan, 1953)), systemic sclerosis (SSc), and systemic lupus erythematoses (SLE). The effects of silica on autoimmunity have also been recognized

Correspondence: Takemi Otsuki, Department of Hygiene, Kawasaki Medical School, 577 Matsushima, Kurashiki 7010192, Japan. Tel: 81-86-462-1111; Fax: 81-86-464-1125; Email: takemi@med.kawasaki-m.ac.jp

following the discovery that patients who receive plastic surgery with implants containing silicone ($[SiO_2\text{-}O\text{-}]_n$) show frequent complications involving autoimmune disorders (Shons and Schubert, 1992; Hirmand et al. 1993). These findings clearly indicate that crystalline silica causes dysregulation and/or disturbance of the human immune system, particularly autoimmunity.

The overall evidence suggests that asbestos may influence human immunocompetent cells and that such alterations may affect the occurrence and progression of asbestos-related malignant diseases. Thus, we have focused on the immunological effects of asbestos. Among the many types of asbestos, chrysotile has mainly been used in our experiments. It is known that magnesium, the main compartment of chrysotile as silicate, usually dissociates from the chrysotile core (SiO_2) in the human body after inhalation, and chrysotile is known to induce malignant transformation. However, its carcinogenic capacity is lower than that of other forms of iron-containing asbestos such as crocidolite and amosite (Harington, 1991).

In this article, we present immunological changes in MM patients with our experimental model. These changes may have resulted from the immunological effects of asbestos on human immunocompetent cells, and may offer some suggestions for the immunological prevention of the occurrence and progression of asbestos-induced malignant diseases.

bcl-2 expression of peripheral CD4+ T cells in MM patients

As shown in the upper panel of Figure 1-A, peripheral CD4+ T cells from MM patients showed a significantly higher expression of *bcl-2* compared to that of healthy volunteers (Miura et al. 2006). This may suggest that the over-expression of *bcl-2* in peripheral CD4+ T cells is one of the markers for the occurrence of MM, although it should be determined whether many cancer-bearing patients respond in a similar manner. The experimental background of this finding is as follows.

Experiments that exposed a high dose of chrysotile to peripheral fresh T cells or T cell-derived cell lines for a short time revealed that a human T-cell leukemia virus type-1 (HTLV-1)-immortalized human polyclonal T-cell line, MT-2, underwent apoptosis with ROS production via activation of the mitochondrial apoptotic pathway with the phosphorylation of p38 mitogen-activated protein kinase (MAPK) and c-Jun N-terminal kinase (JNK) signaling molecules. In addition, we observed a shift of the Bax-dominant Bax/Bcl-2 balance, the release of cytochrome-c from mitochondria into the cytosol, and the activation of caspases 9 and 3 upon short-term, high-level exposure to chrysotile (Hyodoh et al. 2005). However, we thought that an *in vitro* experimental model of chronic exposure was necessary in order to analyze the immunobiological effects of silicates during long-term exposure and to transfer these experimental findings to clinical analyses.

Thus, we established a chrysotile-induced apoptosis-resistant subline of MT-2 (MT-2Rst), and characterized the cell biological differences between the original MT-2 cell line (MT-2Org) and MT-2Rst. MT-2Rst cells were characterized by (i) an enhanced expression of *bcl-2* as shown in the lower panel of Figure 1-A, restoring apoptosis sensitivity with the decrease in *bcl-2* expression level by siRNA, (ii) excessive interleukin (IL)-10 secretion and expression, and (iii) the activation of signal transducers and activators of transcription (STAT) 3 inhibited by 4-amino-5-(4-chlorophenyl)-7-(t-butyl) pyrazolol [3,4-d] pyrimidine (PP2), a specific inhibitor of Src family kinases. These findings suggest that contact between cells and asbestos may affect the human immune system and trigger a cascade of biological events, such as the activation of Src family kinases, enhancement of IL-10 expression, STAT3 activation, and Bcl-2 over-expression as previously reported (Miura et al. 2006).

Another interesting finding was obtained from analyses using *bcl-2* expression in peripheral CD4+ T cells. We performed factor analysis using various clinical parameters and the *bcl-2* relative expression ratio (*bcl-2* RER) obtained by real-time RT-PCR from MM patients. Our results revealed that *bcl-2* RER, a past history of asbestos exposure, peripheral platelet counts, and serum CRP values formed one factor, and these parameters exhibited higher, present, lower count, and lower values, respectively, as shown in Table 1. Platelet-derived growth factor (PDGF) is one of the widely known MM-related growth factors and it functions as the autocrine/paracrine proliferation-promoting factor for mesothelioma cancer cells (Langerak et al. 1996, Klominek et al. 1998). Although higher serum levels of PDGF in MM patients are thought to be produced from mesothelioma cells and *bcl-2*

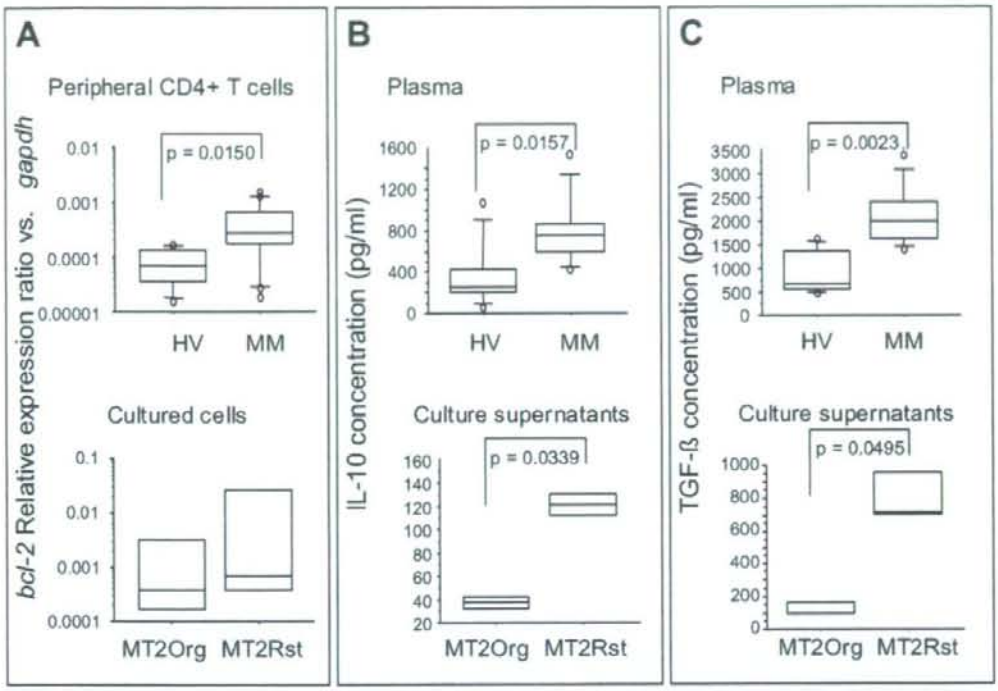

Figure 1. Comparison of *bcl-2* relative expression ratio vs. *gapdh* plasma concentrations in anti-inflammatory cytokines in MM patients and healthy volunteers (HV), and *bcl-2* expression and secretion of these cytokines from experimental low-dose and long-term exposed T-cell models to asbestos (MT-2Org and MT-2Rst, see text for details).

Panel A shows the relative expression ratio of *bcl-2* in peripheral blood CD4+ cells (upper panel) from MM patients and HV, or in cultured MT-2Org and MT-2Rst cells (lower panel). Panels B and C show the plasma concentrations of IL-10 (B) and TGF-ß (C) from MM patients and HV (upper panels), or the concentrations in culture supernatants of IL-10 (B) and TGF-ß (C) from MT-2Org and MT-2Rst cells (lower panels).

Peripheral blood mononuclear cells (PBMCs) were isolated from the heparinized blood of healthy donors and MM patients using a Ficoll-Hypaque density gradient (Separate-L®, Muto Pure Chemicals Co. Ltd., Tokyo, Japan). For the isolation of CD4+ T cells, PBMCs were further separated using Magnetic Cell Separation (MACS) CD4 MicroBeads (Miltenyi Biotech, Bergisch Gladbach, Germany) according to the manufacturer's instructions. The enriched cells were >90% pure as determined by flow cytometry. Specimens were taken from healthy volunteers and patients from whom informed consent had been obtained. The Institutional Ethics Committee of Kawasaki Medical School, Hyogo College of Medicine, and Okayama Rosai Hospital approved the project. A fluorescence thermocycler (Mx3000P® QPCR System, Stratagene Corporation, La Jolla, CA) was used for real-time RT-PCR experiments by following the instructions of the manufacturer. The fluorescence-labeled amplification product is measured continuously with this technique. Total RNA obtained from CD4+ T cells isolated from peripheral CD4+ T cells was extracted using an RNA Bee kit (Tel-Test, Inc., Friendswood, Texas), and 5 µg of RNA was reverse-transcribed with standard methods using a RevertAid™ H Minus First Strand cDNA Synthesis Kit (Fermentas International Inc., Ontario, Canada). An amount of cDNA equivalent to 50 ng of RNA served as the template for PCR in a volume of 20 µl (each primer and SYBER Premix Ex Taq, TaKaRa). The primers for *bcl-2* and *gapdh* were added to the same reaction tube at the optimal concentration for each primer set and PCR was performed. Primers were as follows: *bcl-2*; 5'-TGATGTGAGTCTGGGCTGAG-3' (Forward: Fw) and 5'-GAACGCTTTGTCCAGAGGAG-3' (Reverse: Rv), Bax; 5'-AGTAACATGGAGCTGCAGAGG-3' (Fw) and 5'-ATGGTTCTGATCAGTTCCGG-3' (Rv), *gapdh*; 5'-GAGTCAACGGATTTGGTCGT-3' (Fw) and 5'-TTGATTTTGGAGGGATCTCG-3' (Rv).

The relative expression of various target genes such as *bcl-2* was calculated as follows when real-time RT-PCR was performed: [A: number of PCR cycles required to reach a certain intensity of fluorescence for the *gapdh* product. B: number of PCR cycles required to reach the same fluorescent intensity for the target gene product (*bcl-2*) derived from the same sample.] The relative level of the target gene is expressed as 1/2[B-A], with gapdh expression being 1.0. PCR products were confirmed to be successfully amplified by standard agarose gel electrophoresis and staining with ethidium bromide. Comparisons of the results for relative gene expression and proliferation assayed by real-time RT-PCR were analyzed using the Mann-Whitney U-test.

Cytokines in plasma from MM patients and HV and culture supernatant were measured using an ELISA kit (Quantikine® Human TGF-ß1 (or IL-10) Immunoassay; R&D Systems) and the Cytometric Bead Array of Human Th1/Th2 cytokine kit II (CBA, BD Bioscience, San Jose, CA, U.S.A.), and measurements were made using FACSCalibur flow-cytometry (BD Bioscience) according to the manufacturer's instructions.

Table 1. Factor analysis of clinical parameters in mesothelioma patients with relative *bcl-2* expression in peripheral CD4+ T cells.

Parameter	Value (a value of more than ± 0.4 is thought to contribute to the formation of this factor)
bcl-2 relative expression ratio in peripheral CD4+ T cells	**0.59009**
Histology (numbered) epithelial type = 1 mixed type = 2 sarcomatous type = 3	–0.14234
Past asbestos exposure (numbered) existence = 1 unknown = 2 none = 3	**0.55496**
White Blood Cell count	0.22054
Platelet count	**–0.76064**
Concentration of serum creatinine	0.21269
Concentration of serum CRP	**–0.79789**
Contribution rate	**19.18%**

RER is a marker of T cells chronically exposed to asbestos, these may be unknown biological mechanisms between immunocompetent cells with chronic exposure to asbestos and peripheral platelet counts via PDGF.

IL-10 and TGF-ß concentrations in MM patients and the experimental model

As shown in the upper panels of Figures 1-B and 1-C, plasma concentrations of IL-10 and transforming growth factor (TGF)-ß were significantly higher in MM patients than in healthy volunteers. TGF-ß is known as one of the mesothelioma cell-producing cytokines (Gerwin et al. 1987; Maeda et al. 1994). However, the above-mentioned MT-2Rst cells, representing the outcome of the experimental low-dose and long-term asbestos-exposure T-cell model, showed significantly higher secretion of TGF-ß than MT-2Org cells (lower panel of Fig. 1-C). As we mentioned previously, the IL-10 concentration in culture supernatants of MT-2Rst was higher than that of MT-2Org (lower panel of Fig. 1-B). Thus, the source of the elevated TGF-ß and IL-10 concentrations in MM patients is not only tumor cells, but also immunocompetent cells.

It is interesting to note that IL-10 and TGF-ß are the important soluble factors necessary for the function of CD4+25+FoxP3+ regulatory T cells (Treg), even though cell-cell contact is the main route for the manifestation of Treg function (Wahl et al. 2004; Romagnasi, 2006). If circulating Treg and tumor-infiltrated Treg have enhanced function as a result of these elevated concentrations of IL-10 and TGF-ß, further aggressive progression of asbestos-induced cancer cells may have occurred. It may be important to analyze the Treg function using the experimental model that we have developed.

T-cell receptor (TcR) Vß expression

We reported previously that asbestos may act on peripheral T cells as a superantigen (Aikoh et al. 1998; Ueki, 2001). The effects of a superantigen such as staphylococcal enterotoxin B (SEB) may modify TcRVß on peripheral T cells to enhance multiple, but not clonal, TcRVß expression (Schubert, 2001; Li et al. 1999). As shown in Figure 2, various TcRVßs were over-expressed in MM and asbestosis patients. TcRVßs from most patients showed a higher expression, exceeding the average plus 2SD (standard deviation) limit. In addition, several TcRVßs such as Vß 1, 4 and 9 among the 24 kinds of TcRVß were strongly over-expressed in many patients. This phenomenon was also observed from the comparison of TcRVß expression in MT-2Org and MT-2Rst cell lines. As a result, MT-2Rst cells over-expressed various TcRVßs. Although TcRVß-overexpressing MT-2Org cells underwent apoptosis due to their first contact with chrysotile, MT-2Rst cells showed no significant changes when they again came in contact with chrysotile (Nishimura et al. 2006). These findings may suggest that the over-expression of various TcRVßs may be the result of contact between cells and chrysotile, an asbestos fiber, during the acquisition of resistance to CB-induced apoptosis caused by a long-term and low-dose exposure to CB (Nishimura et al. 2006).

The multiple over-expression of TcRVß in CD3+ peripheral T cells derived from asbestos-exposed patients may be one of the candidates to detect previous asbestos exposure. Although these

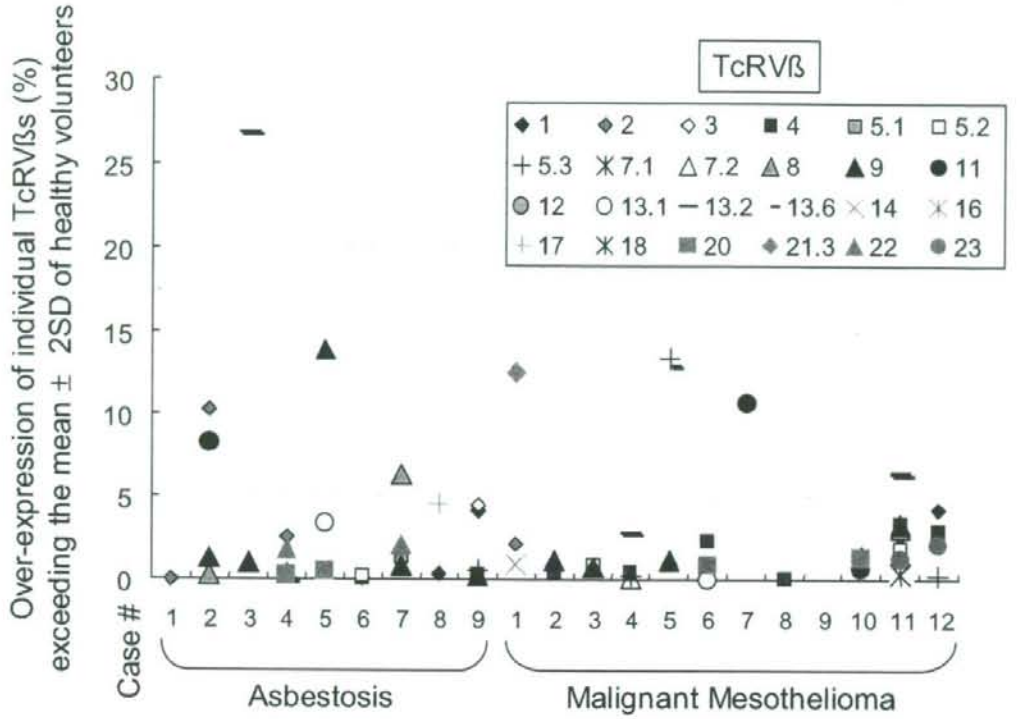

Figure 2. TcRVß expression among patients with asbestosis and malignant mesothelioma. Peripheral blood mononuclear cells (PBMCs) were obtained from 6 HV (mean age ± SD, 38.0 ± 6.4 years old; male(M):female(F),1:5), 9 asbestosis patients without significant clinical signs of complications such as lung cancer or malignant mesothelioma (ASB; 74.4 ± 3.9, all males), and 12 patients with malignant mesothelioma (MM; 58.7 ± 10.1, M:F, 9:3). Specimens were only taken once informed consent had been obtained. The study was approved by the Ethics Committee of Kawasaki Medical School, Okayama Rosai Hospital, Hyogo College of Medicine and Kusaka Hospital. The expression of TcRVß in CD3+ cells derived from HV, ASB and MM subjects was examined with an IOTest Beta Mark TcRVß repertoire analysis kit (Beckman Coulter, Inc., Fullerton, CA) using a FACSCalibur flow cytometer (Becton, Dickinson and Company, Franklin Lakes, NJ) according to the manufacturer's instructions. This kit can analyze TcRVß 1, 2, 3, 4, 5.1, 5.2, 5.3, 7.1, 7.2, 8, 9, 11, 12, 13.1, 13.2, 13.6, 14, 16, 17, 18, 20, 21.3, 22 and 23 from 1 ml of peripheral blood. The 0% expression in this figure is the mean + 2SD for HV. Thus, each symbol indicates the number of over-expressions observed in individual patients for individual TcRVßs.

data were obtained from a limited number of patients, it is worth continuing these analyses using samples from many patients in an effort to explore the biological mechanisms involved in these findings.

Conclusion

A summarized schematic presentation of various aspects of this investigation is shown in Figure 3. This schema only shows the experimental and clinical findings related to asbestos exposure of T cells. We have been investigating the effects of asbestos on the function of natural killer (NK) cells from cellular and molecular viewpoints. TGF-ß is similar to PDGF in that it is also known as a mesothelioma-producing growth factor (Gerwin et al. 1987; Maeda et al. 1994; Langerak et al. 1996; Klominek et al. 1998). Thus, the effects of TGF-ß1 on asbestos-exposed MT-2Rst cells are being investigated and compared with MT-2Rst and MT-2Org cells that have not been exposed to TGF-ß1. These examinations are on-going and will be presented in the near future.

Recent advances in immunomolecular studies have led to detailed analyses of the immunological effects of asbestos. Asbestos affects immunocompetent cells and these effects may be associated with the pathophysiological development of complications in asbestos-exposed patients such as malignant tumors. In addition, immunological analyses may lead to the discovery of new clinical tools for the modification of pathophysiological

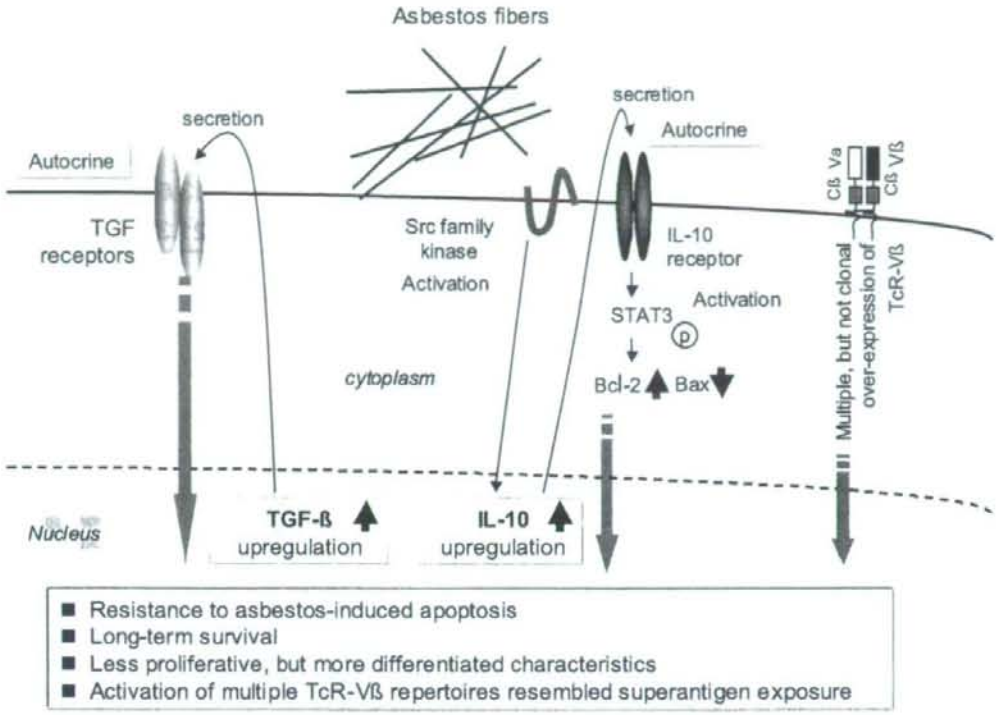

Figure 3. Experimental findings of immunological effects of chrysotile, a form of asbestos, induced by long-term and low-dose exposure using MT-2, an HTLV-1 immortalized human polyclonal T-cell line.

aspects of diseases, such as the regulation of tumor immunity using cell-mediated therapies, various cytokines and molecule-targeting therapies. As the incidence of asbestos-related malignancies increases against the growing concern in Japan since the summer of 2005 for medical and social problems created by such malignancies, efforts should be focused on developing a cure for these diseases in order to eliminate the nationwide anxiety concerning these malignancies.

Acknowledgements

The authors thank Ms. Misao Kuroki, Keiko Kimura, Tomoko Sueishi, Yoshiko Yamashita, Keiko Kimkura, Satomi Hatada, Yumika Isozaki and Haruko Sakaguchi for technical assistance.

The data obtained in the Department of Hygiene, Kawasaki Medical School and published by the authors were supported by Special Coordination Funds for Promoting Science and Technology (H18-1-3-3-1), JSPS KAKENHI (17790375, 18390186, 19689153, 19790431 and 19790411), Kawasaki Medical School Project Grants (16-212, 16-401N, 17-210S, 7-404M, 17-611O, 18-209T, 18-403 and 18-601), a Sumitomo Foundation Grant (053027), and a Yasuda Memorial Foundation Grant (H18).

References

Aikoh, T., Tomokuni, A., Matsukii, T. et al. 1998. Activation-induced cell death in human peripheral blood lymphocytes after stimulation with silicate in vitro. *Int. J. Oncol.*, 12:1355–9.

Becklake, M.R., Bagatin, E. and Neder, J.A. 2007. Asbestos-related diseases of the lungs and pleura: uses, trends and management over the last century. *Int. J. Tuberc. Lung Dis.*, 11:356–69.

Caplan, A. 1953. Certain unusual radiological appearances in the chest of coal-miners suffering from rheumatoid arthritis. *Thorax*, 8(1):29–37.

Cooper, G.S. and Parks, C.G. 2004. Occupational and environmental exposures as risk factors for systemic lupus erythematosus. *Curr. Rheumatol. Rep.*, 6(5):367–74.

Gerwin, B.I., Lechner, J.F., Reddel, R.R. et al. 1987. Comparison of production of transforming growth factor-beta and platelet-derived growth factor by normal human mesothelial cells and mesothelioma cell lines. *Cancer Res.*, 47:6180–4.

Harington, J.S. 1991. The carcinogenicity of chrysotile asbestos. *Ann. N.Y. Acad. Sci.*, 31(643):465–72.

Hess, E.V. 2002. Environmental chemicals and autoimmune disease: cause and effect. *Toxicology*, 181(182):65–70.

Hirmand, H., Latrenta, G.S. and Hoffman, L.A. 1993. Autoimmune disease and silicone breast implants. *Oncology* (Williston Park), 7:17–24.

Hyodoh, F., Takata-Tomokuni, A., Miura, Y. et al. 2005. Inhibitory effects of anti-oxidants on apoptosis of a human polyclonal T-cell line, MT-2, induced by an asbestos, chrysotile-A. Scand *J. Immunol.*, 61:442–8.

Kanazawa, N., Ioka, A., Tsukuma, H. et al. 2006. Incidence and survival of mesothelioma in Osaka, Japan. *Jpn. J. Clin. Onco.*, 36:254–7.

Klominek, J., Baskin, B. and Hauzenberger, D. 1998. Platelet-derived growth factor (PDGF) BB. acts as a chemoattractant for human malignant mesothelioma cells via PDGF receptor beta-integrin alpha3beta1 interaction. *Clin. Exp. Metastasis*, 16:529–39.

Langerak, A.W., De Laat, P.A., Van Der Linden-Van Beurden, C.A. et al. 1996. Expression of platelet-derived growth factor (PDGF) and PDGF receptors in human malignant mesothelioma in vitro and in vivo. *J. Pathol.*, 178:151–60.

Li, H., Llera, A., Malchiodi, E.L. et al. 1999. The structural basis of T cell activation by superantigens. *Annu. Rev. Immunol.*, 17:435–66.

Maeda, J., Ueki, N., Ohkawa, T. et al. 1994. Transforming growth factor-beta 1 (TGF-beta 1)- and beta 2-like activities in malignant pleural effusions caused by malignant mesothelioma or primary lung cancer. *Clin. Exp. Immunol.*, 98:319–22.

Miura, Y., Nishimura, Y., Katsuyama, H. et al. 2006. Involvement of IL-10 and Bcl-2 in resistance against an asbestos-induced apoptosis of T cells. *Apoptosis*, 11:1825–35.

Murayama, T., Takahashi, K., Natori, Y. et al. 2006. Estimation of future mortality from pleural malignant mesothelioma in Japan based on an age-cohort model. *Am. J. Ind. Med.*, 49:1–7.

Nakano, T. 2006. Malignant Mesothelioma: Incidence and clinical approach. *Biomed. Res. Trace Elements*, 17:104–6.

Niklinski, J., Niklinska, W., Chyczewska, E. et al. 2004. The epidemiology of asbestos-related diseases. *Lung Cancer*, 45:S7–15.

Nishimura, Y., Miura, Y., Maeda, M. et al. 2006. Expression of the T cell receptor Vbeta repertoire in a human T cell resistant to asbestos-induced apoptosis and peripheral blood T cells from patients with silica and asbestos-related diseases. *Int. J. Immunopathol. Pharmacol.*, 19:795–805.

O'Reilly, K.M., Mclaughlin, A.M., Beckett, W.S. et al. 2007. Asbestos-related lung disease. *Am. Fam Physician*, 75:683–8.

Romagnani, S. 2006. Regulation of the T cell response. *Clin. Exp. Allergy*, 36:1357–66.

Schubert, M.S. 2001. A superantigen hypothesis for the pathogenesis of chronic hypertrophic rhinosinusitis, allergic fungal sinusitis, and related disorders. *Ann. Allergy Asthma Immunol.*, 87:181–8.

Shons, A.R. and Schubert, W. 1992. Silicone breast implants and immune disease. *Ann. Plast. Surg.*, 28:491–501.

Shukla A, Gulumian M, Hei TK, et al. Multiple roles of oxidants in the pathogenesis of asbestos-induced diseases. *Free Radic. Biol. Med.*, 34:1117–29.

Shukla, A., Jung, M., Stern, M. et al. 2003. Asbestos induces mitochondrial DNA damage and dysfunction linked to the development of apoptosis. *Am. J. Physiol. Lung Cell Mol. Physiol.*, 285:L1018–25.

Tsiouris, A. and Walesby, R.K. 2007. Malignant pleural mesothelioma: current concepts in treatment. *Nat. Clin. Pract. Oncol.*, 4:344–52.

Ueki, A. 2001. Biological effects of asbestos fibers on human cells in vitro – especially on lymphocytes and neutrophils. *Indust. Health*, 39:84–93.

Upadhyay, D. and Kamp, D.W. 2003. Asbestos-induced pulmonary toxicity: role of DNA damage and apoptosis. *Exp. Biol. Med* (Maywood), 228:650–9.

Vogelzang, N. and Pass, H.I. 2006. Newer issues in mesothelioma chemotherapy. *J. Thorac. Oncol.*, 1:177–9.

Wahl, S.M., Swisher, J., McCartney-Francis, N. et al. 2004. TGF-beta: the perpetrator of immune suppression by regulatory T cells and suicidal T cells. *J. Leukoc. Biol.*, 76:15–24.

Zucali, P.A. and Giaccone, G. 2006. Biology and management of malignant pleural mesothelioma. *Eur. J. Cancer*, 42:2706–14.

Environ Health Prev Med (2008) 13:55–59
DOI 10.1007/s12199-007-0012-y

Immunological alterations found in mesothelioma patients and supporting experimental evidence

Yoshie Miura · Yasumitsu Nishimura · Megumi Maeda · Shuko Murakami · Hiroaki Hayashi · Kazuya Fukuoka · Takumi Kishimoto · Takashi Nakano · Takemi Otsuki

Received: 27 June 2007 / Accepted: 31 July 2007 / Published online: 28 February 2008

Abstract It is common knowledge that exposure to asbestos causes asbestos-related diseases, such as asbestosis, lung cancer and malignant mesothelioma, not only in people who have had long-term contact with asbestos in their work environment but also in residents living near factories that handle asbestos. Since the summer of 2005, these revelations turned into a large medical problem and caused and social unrest. We have focused on the immunological effects of both asbestos and silica on the human immune system. In this brief review, we introduce immunological alterations found in patients with malignant mesothelioma and describe the experimental background in which these were found. Analyzing the immunological effects of asbestos may improve our understanding of the biological effects of asbestos.

Keywords Asbestos · Chrysotile · Immunology · Mesothelioma

Y. Miura · Y. Nishimura · M. Maeda · S. Murakami · H. Hayashi · T. Otsuki (✉)
Department of Hygiene, Kawasaki Medical School,
577 Matsushima, Kurashiki 701-0192, Japan
e-mail: takemi@med.kawasaki-m.ac.jp

K. Fukuoka · T. Nakano
Department of Respiratory Medicine,
Hyogo Medical College of Medicine,
1-1 Mukogawa-cho, Nishinomiya 663-8131, Japan

T. Kishimoto
Okayama Rosai Hospital,
1-10-25 Chikkou-midori-machi,
Okayama 702-8055, Japan

Introduction

Asbestos is a generic name for a group of silicate minerals (complexes containing metals, such as iron and magnesium), the most common of which are chrysotile, crocidolite, and amosite. Patients exposed to asbestos develop pulmonary fibrosis, commonly called asbestosis, mesothelial plaque and malignant diseases, such as lung cancer and malignant mesothelioma (MM) [1–3]. Some of these malignancies may be considered to be a result of a decline in tumor immunity owing to the exposure of immunocompetent cells to asbestos.

Silica is known to be one of the most hazardous environmental substances in terms of causing autoimmunity dysfunction [4–6]. Silicosis patients often develop immunological complications, such as rheumatic arthritis (known as Caplan syndrome; [7–9], systemic sclerosis (SSc) and systemic lupus erythematoses (SLE). The effects of silica on autoimmunity have also been assumed as patients who receive plastic surgery with implants containing silicone ($[SiO_2–O–]_n$) also frequently develop complications related to autoimmune disorders [10–12]. Taken together, these findings clearly indicate that crystalline silica causes dysregulation and/or disturbance of the human immune system in general, and of autoimmunity in particular.

Asbestos may affect human immunocompetent cells, and these alterations may, in turn, influence the occurrence and progression of asbestos-related malignant diseases, such as MM. For this reason, this article focuses on the immunological effects of asbestos. Chrysotile has been the most commonly used type of asbestos in our experiments. Magnesium, the main compartment of chrysotile as a silicate, usually dissociates from the chrysotile core, SiO_2, in the human body

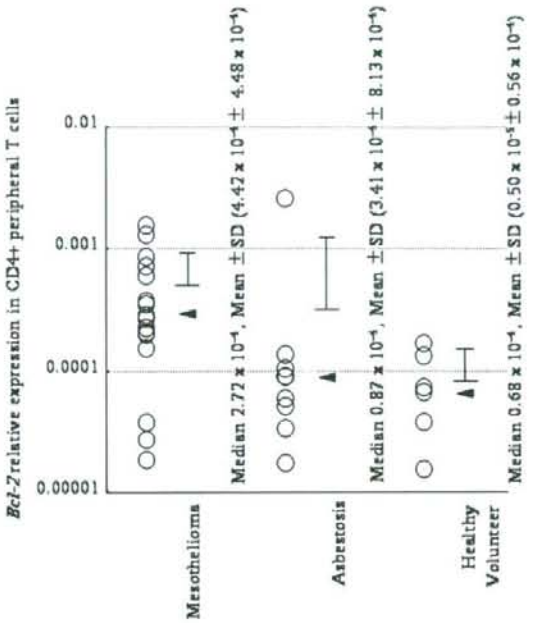

Fig. 1 Comparison of *bcl-2* relative expression ratio (RER) in peripheral blood CD4+ T cells among healthy volunteers, asbestosis patients and malignant mesothelioma (MM) patients. Peripheral blood mononuclear cells (PBMCs) were isolated from heparinized blood of healthy donors and from patients with asbestosis and MM using a Ficoll–Hypaque density gradient (Separate-L; Muto Pure Chemicals, Tokyo, Japan). For the isolation of CD4+ T cells, PBMCs were further separated using magnetic cell separation (MACS) CD4 MicroBeads (Miltenyi Biotech, Bergisch Gladbach, Germany) according to the manufacturer's instructions. The enriched cells were >90% pure as determined by flow cytometry. Specimens were taken from healthy volunteers and patients from whom informed consent had been obtained. The Institutional Ethics Committee of Kawasaki Medical School, Hyogo College of Medicine, and Okayama Rosai Hospital approved the project. A fluorescence thermocycler (Mx3000P QPCR System; Stratagene, La Jolla, CA) was used for real-time reverse transcriptase (RT)-PCR experiments following the instructions of the manufacturer. With this technique, the fluorescence-labeled amplification product is measured continuously. Total RNA obtained from CD4+ T cells isolated from peripheral CD4+ T cells was extracted using an RNA Bee kit (Tel-Test, Friendswood, TX), and 5 μg of RNA was reverse-transcribed with standard methods using a RevertAid H Minus First Strand cDNA Synthesis lit (Fermentas, Ontario, Canada). An amount of cDNA equivalent to 50 ng of RNA served as the template for PCR in a volume of 20 μl (each primer and SYBER Premix Ex Taq; TaKaRa, Japan). The primers for *bcl-2* and *gapdh* were added to the same reaction tube at the optimal concentration for each primer set, and PCR was performed. The primers were as follows: Bcl-2 [5′-TGATGTGAG TCTGGGCTGAG-3′ (forward: Fw) and 5′-GAACGCTTTGTCCA GAGGAG-3′ (reverse, Rv)]; Bax [5′-AGTAACATGGAGCTGCA GAGG-3′ (Fw) and 5′-ATGGTTCTGATCAGTTCCGG-3′ (Rv)]; GAPDH [5′-GAGTCAACGGATTTGGTCGT-3′ (Fw) and 5′-TTGA TTTTGGAGGGATCTCG-3′ (Rv)]. The relative expression of various target genes, such as *bcl-2*, was calculated when real-time RT-PCR was performed. The relative level of the target gene is expressed as $½[B - A]$, with *gapdh* expression being 1.0, and A = number of PCR cycles required to reach a certain intensity of fluorescence for the *gapdh* product, and B = number of PCR cycles required to reach the same fluorescent intensity for the target gene product (*bcl-2*) derived from the same sample. PCR products were confirmed to be successfully amplified by standard agarose gel electrophoresis and staining with ethidium bromide. Comparisons of the results for relative gene expression and proliferation assayed by real-time RT-PCR were analyzed using Fisher's parametric least significant difference (PLSD) test

after inhalation. Chrysotile is known to induce malignant transformation, but its carcinogenic capacity is lower than that of iron-containing asbestos, such as crocidolite and amosite [13–15].

We report here the immunological alterations of MM patients in an experimental background. These changes may have resulted from the immunological effects of asbestos on human immunocompetent cells and, as such, may provide valuable information that can be used in preventing the immunological changes seen in the occurrence and progression of asbestos-induced malignant diseases.

bcl-2 expression of peripheral CD4+ T cells in MM patients

Figure 1 shows that peripheral CD4+ T cells from MM patients express significantly more *bcl-2* than healthy volunteers and asbestosis patients [16]. This may suggest that the overexpression of *bcl-2* in peripheral CD4+ T cells is one of the markers of the occurrence of MM in asbestos-exposed patients, although further study is necessary to determine whether many other cancer-bearing patients show the same change. The experimental background leading up to this finding is as follows.

We first exposed peripheral fresh T cells or T cell-derived cell lines to high doses of chrysotile for a short time and found that a human T-cell leukemia virus type-1 (HTLV-1)-immortalized human polyclonal T cell line, MT-2, underwent apoptosis. This apoptosis progressed with reactive oxygen species (ROS) production via activation of the mitochondrial apoptotic pathway with the phosphorylation of p38 mitogen-activated protein kinase (MAPK) and c-Jun N-terminal kinase (JNK) signaling molecules. In addition, short-term, high-level exposure to chrysotile resulted in a shift of the Bax-dominant Bax/Bcl-2 balance followed by the release of cytochrome-c from mitochondria into the cytosol and the activation of caspases 9 and 3 [17]. These observations led us to believe that an in vitro experimental model of chronic exposure was necessary both to analyze the immunobiological effects of

silicates during long-term exposure and to be able to extrapolate these experimental findings to clinical analyses.

We therefore established a chrysotile-induced apoptosis-resistant subline of MT-2 (MT-2Rst) and characterized the cell biological differences between the original MT-2 cell line (MT-2Org) and MT-2Rst. MT-2Rst cells were characterized by (1) an enhanced expression of *bcl-2*, restoring apoptosis sensitivity with the decrease in *bcl-2* expression level by siRNA, (2) excessive IL-10 secretion and expression and (3) the activation of STAT3 inhibited by 4-amino-5-(4-chlorophenyl)-7-(*t*-butyl) pyrazolol [3,4-*d*] pyrimidine (PP2), a specific inhibitor of the Src family kinases. These findings suggest that contact between cells and asbestos may affect the human immune system and trigger a cascade of biological events, such as the activation of Src family kinases, enhancement of IL-10 expression, STAT3 activation and Bcl-2 overexpression, as previously reported [16].

Another interesting finding was obtained from analyses using *bcl-2* expression in peripheral CD4+ T cells. We performed factor analysis using various clinical parameters and individual *bcl-2* relative expression ratios (*bcl-2* RER) obtained by real-time RT-PCR from MM patients. This analysis revealed that *bcl-2* RER, a past history of asbestos exposure, peripheral platelet counts and serum CRP values formed one factor and that each parameter was related as higher, present, lower count, and lower value, respectively, as shown in Table 1. Platelet-derived growth factor (PDGF) is one of the most known mesothelioma-related growth factors, and it functions as the autocrine/paracrine proliferation-promoting factor for mesothelioma cancer cells [18–21]. Although higher serum levels of PDGF in MM patients are thought to be produced from mesothelioma cells and *bcl-2* RER is a known marker of T cells chronically exposed to asbestos, there may be unknown biological mechanisms between immunocompetent cells with chronic exposure to asbestos and peripheral platelet counts via PDGF.

Table 1 Factor analysis in clinical parameters of mesothelioma patients with relative *bcl-2* expression in peripheral CD4+ T cells

Parameter	Value (value more than ±0.4 is considered to contribute to form this factor)
bcl-2 relative expression ratio in peripheral CD4+ T cells	**0.59009**
Histology (numbered)	−0.14234
Epithelial type = 1	
Mixed type = 2	
Sarcomatous type = 3	
Past asbestos exposure (numbered)	**0.55496**
Existence = 1	
Unknown = 2	
None = 3	
Count of WBC	0.22054
Count of platelets	**−0.76064**
Concentration of serum creatinin	0.21269
Concentration of serum CRP	**−0.79789**
Contribution rate	**19.18%**

T cell receptor (TCR)Vβ expression

We have previously reported that asbestos may act on peripheral T cells as a superantigen [22–24]. The effects of a superantigen, such as staphylococcal enterotoxin B (SEB), may modify TCRVβ on peripheral T cells to enhance multiple, but not clonal, TCRVβ expression [25–28]. As shown in Fig. 2, various TCRVβs were overexpressed in MM and asbestosis patients. There was a higher expression

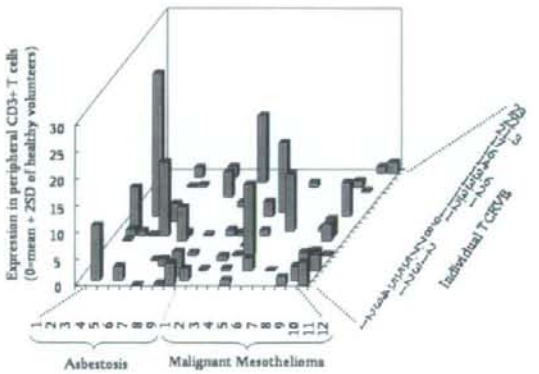

Fig. 2 T cell receptor (TCR)Vβ expression among patients with asbestosis and MM. Peripheral blood mononuclear cells were obtained from six healthy volunteers [HV; mean age ± SD: 38.0 ± 6.4 years; male (M):female (F): 1:5], nine asbestosis patients without significant clinical signs of complications, such as lung cancer or malignant mesothelioma (ASB; 74.4 ± 3.9; all males) and 12 patients with MM (58.7 ± 10.1; M:F: 9:3). Specimens were taken only once informed consent had been obtained. The study was approved by the Ethics Committee of Kawasaki Medical School, Okayama Rosai Hospital, Hyogo College of Medicine and Kusaka Hospital. The expression of TCRVβ in CD3+ cells derived from HV, ASB and MM subjects was examined with an IOTest Beta Mark TCRVβ repertoire analysis kit (Beckman Coulter, Fullerton, CA) using a FACSCalibur flowcytometer (Becton, Dickinson and Company, Franklin Lakes, NJ) according to the manufacturer's instructions. This kit can analyze TcRVβ1, -2, -3, -4, -5.1, -5.2, -5.3, -7.1, -7.2, -8, -9, -11, -12, -13.1, -13.2, -13.6, -14, -16, -17, -18, -20, -21.3, -22 and -23 from 1 ml of peripheral blood. The 0% expression in this figure is the mean + 2 SD of HV. Thus, each *bar* indicates how many overexpressions were observed in individual patients and individual TVRVβs